Navigation of Nonholonomic Mobile Robot Using Visual Potential Field

Naoya Ohnishi[1] and Atsushi Imiya[2]

[1] School of Science and Technology, Chiba University, Japan
Yayoicho 1-33, Inage-ku, Chiba, 263-8522, Japan
ohnishi@graduate.chiba-u.jp
[2] Institute of Media and Information Technology, Chiba University, Japan
Yayoicho 1-33, Inage-ku, Chiba, 263-8522, Japan
imiya@faculty.chiba-u.jp

Abstract. In this paper, we develop an algorithm for the navigation of a nonholonomic mobile robot using the visual potential. The robot is equipped with a camera system which dynamically captures the environment. The visual potential is computed from an image sequence and optical flow computed from successive images captured by the camera mounted on the robot. Our robot selects a local pathway using the visual potential computed from its vision system without any knowledge of a robot workspace. We present experimental results of the obstacle avoidance in the real environment.

Key words: Robot navigation, Potential field, Optical flow

1 Introduction

Recently, the control systems for autonomous mobile robots are actively studied, since mobile robots are widely used in various environments, for example, at factories, in the office, and home. In such environments, the robot needs to move safely without collision with obstacles and walls. If the robot has the environmental map, the potential field method [11] is a valid method of path planning. In the real world, however, the robot might not have the environmental map, and the environments dynamically change [20]. Furthermore, many of mobile robots in the real environment are wheel driven robots, and it moves by a nonholonomic mechanism [6, 13]. In this paper, we propose an algorithm for the autonomous-mobile-robot navigation using the visual potential field. The visual potential field is computed from an image sequence captured by the camera mounted on the mobile robot. Our algorithm enables the mobile robot to navigate without collision with obstacles. In the real environment, the payload of a mobile robot is restricted, for example, power supply, capacity of input devices and computing power. Therefore, mobile robots are required to have simple mechanisms and devices [8, 16]. We use an uncalibrated monocular camera as a sensor for obtaining information on the environment. This vision sensor is a low-cost device that is

Proceedings of the 5th International Conference on Computer Vision Systems (ICVS 2007)
Published in 2007 by Applied Computer Science Group, Bielefeld University, Germany, ISBN 978-3-00-020933-8
This document and other contributions archived and available at: http://biecoll.ub.uni-bielefeld.de

easily mounted on mobile robots. Therefore, we use visual information for the mobile robot navigation.

In recent years, the navigation systems of the nonholonomic mobile robot using vision systems [4, 14, 22] are widely studied. A two-wheeled robot, which is addressed in our work, is a typical nonholonomic mobile system. In the previous works [19], visual information is used as the control parameters for tracking of pre-determined trajectories. Therefore, they [19] implemented the visual servo system for the trajectory control of a nonholonomic mobile robot. In this paper, we, however, use visual information for the collision-free navigation of the robot without any pre-determined robot trajectories.

The potential field method [11] is an established method of path planning for the mobile robots. In this method, the potential field is generated from the terrain and the configuration of obstacles in a workspace [1, 18, 21]. In this case, the potential field method for path planning is a model-based robot-control method. Usually, an attractive force to the destination and a repulsive force from obstacles are generated to guide the robot to the destination without collision with the obstacles in the robot workspace [5, 19]. Basically, these two guiding forces are generated from the terrain and the obstacle configuration in the workspace, which are usually pre-input to the robot.

The visual potential field on an image is an approximation of the projection of the potential field in the workspace to the image plane. Accepting this potential, the robot navigates by referring to a sequence of images without using the spatial configuration of obstacles. Then, we use the optical flow field [2, 10, 12, 15] as the guiding force field to the destination of the robot, since the flow vectors indicate the direction of robot motion to a local destination. Furthermore, using images captured by the camera mounted on the robot, the potential field for the repulsive force from obstacles is generated to avoid collision. We call the potential generated on an image the visual potential. Using the visual potential field and optical flow, we define a control flow for the mobile robot, as shown in Fig. 1.

In section 2, we briefly overview our featureless method for detecting the dominant plane using optical flow. Section 3 is devoted to the introduction of the visual potential field and the definition of the control force computed from the visual field. Section 4, we show implementation of our algorithm into a mobile robot. In section 5, we present some experimental results of robot navigation.

2 Dominant Plane Detection from Optical Flow

Setting $I(x, y, t)$ and $(\dot{x}, \dot{y})^\top$ to be the time-varying gray-scale-valued image at time t and optical flow, optical flow $(\dot{x}, \dot{y})^\top$ at each point $(x, y)^\top$ satisfies

$$\frac{\partial I}{\partial x}\dot{x} + \frac{\partial I}{\partial y}\dot{y} + \frac{\partial I}{\partial t} = 0. \tag{1}$$

The computation of $(\dot{x}, \dot{y})^\top$ from $I(x, y, t)$ is an ill-posed problem, Therefore, additional constraints are required to compute $(\dot{x}, \dot{y})^\top$. We use the Lucas-Kanade method with pyramids [3].

Proceedings of the 5th International Conference on Computer Vision Systems (ICVS 2007)
Published in 2007 by Applied Computer Science Group, Bielefeld University, Germany, ISBN 978-3-00-020933-8
This document and other contributions archived and available at: http://biecoll.ub.uni-bielefeld.de

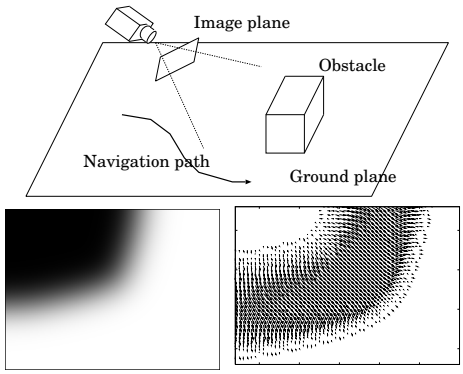

Fig. 1. Visual potential in a robot workspace. By our method, a navigation path without collision with obstacles is derived without the need for an environmental map. (Top) Configuration of robot workspace. (Bottom left) Image captured by the camera mounted on the mobile robot. (Bottom right) Repulsive force from the obstacle

We define the dominant plane as a planar area in the world corresponding to the largest part in an image. Assuming that the dominant plane in an image corresponds to the ground plane on which the robot moves, the detection of the dominant plane enables the robot to detect the feasible region for navigation in its workspace.

Setting $\boldsymbol{H}$ to be a 3×3 matrix [9], the homography between the two images of a planar surface can be expressed as

$$(x', y', 1)^\top = \boldsymbol{H}(x, y, 1)^\top, \tag{2}$$

where $(x, y, 1)^\top$ and $(x', y', 1)^\top$ are homogeneous coordinates of corresponding points in two successive images. Assuming that the camera displacement is small, matrix $\boldsymbol{H}$ is approximated by affine transformations. These geometrical and mathematical assumptions are valid when the camera is mounted on a mobile robot moving on the dominant plane. Therefore, the corresponding points $\boldsymbol{p} = (x, y)^\top$ and $\boldsymbol{p'} = (x', y')^\top$ on the dominant plane are expressed as

$$\boldsymbol{p'} = \boldsymbol{A}\boldsymbol{p} + \boldsymbol{b}, \tag{3}$$

where $\boldsymbol{A}$ and $\boldsymbol{b}$ are a 2×2 affine-coefficient matrix and a 2-dimensional vector, which are approximations of $\boldsymbol{H}$.

Therefore, we can estimate the affine coefficients using the RANSAC-based algorithm [7, 9, 17]. Using estimated affine coefficients, we can estimate optical flow on the dominant plane $(\hat{x}, \hat{y})^\top$,

$$(\hat{x}, \hat{y})^\top = \boldsymbol{A}(x, y)^\top + \boldsymbol{b} - (x, y)^\top, \tag{4}$$

for all points $(x, y)^\top$ in the image. We call $(\hat{x}, \hat{y})^\top$ *planar flow*, and $\hat{\boldsymbol{u}}(x, y, t)$ *planar flow field* at time t, which is a set of planar flow $(\hat{x}, \hat{y})$ computed for all pixels in an image.

Proceedings of the 5th International Conference on Computer Vision Systems (ICVS 2007)
Published in 2007 by Applied Computer Science Group, Bielefeld University, Germany, ISBN 978-3-00-020933-8
This document and other contributions archived and available at: http://biecoll.ub.uni-bielefeld.de

If an obstacle exist in front of the robot, the planar flow on the image plane differs from the optical flow on the image plane. Since the planar flow $(\hat{x}, \hat{y})^\top$ is equal to the optical flow $(\dot{x}, \dot{y})^\top$ on the dominant plane, we use the difference between these two flows to detect the dominant plane. We set ε to be the tolerance of the difference between the optical flow vector and the planar flow vector. Therefore, if

$$\left|(\dot{x}, \dot{y})^\top - (\hat{x}, \hat{y})^\top\right| < \varepsilon \tag{5}$$

is satisfied, we accept the point $(x, y)^\top$ as a point on the dominant plane. Then, the image is represented as a binary image by the dominant plane region and the obstacle region. Therefore, we set $d(x, y, t)$ to be the dominant plane, as

$$d(x, y, t) = \begin{cases} 255, \text{ if } (x, y)^\top \text{ is on the dominant plane} \\ 0, \quad \text{if } (x, y)^\top \text{ is on the obstacle area} \end{cases}.$$

We call $d(x, y, t)$ the dominant plane image.

3 Determination of Robot Motion Using Visual Potential

In this section, we describe the algorithm used for the determination of robot motion from the dominant plane image $d(x, y, t)$ and the planar flow field $\hat{\boldsymbol{u}}(x, y, t)$.

3.1 Gradient Vector of Image Sequence

Since the dominant plane image $d(x, y, t)$ is a binary image sequence, the computation of the gradient is numerically unstable and unrobust. Therefore, as a preprocess to the computation of the gradient, we smooth the dominant plane image $d(x, y, t)$ by convolution with Gaussian $G = \frac{1}{2\pi\sigma} e^{-\frac{x^2+y^2}{2\sigma^2}}$, that is, we adopt $\boldsymbol{g}$ such that

$$\boldsymbol{g}(x, y, t) = \nabla(G * d(x, y, t)) = \begin{pmatrix} \frac{\partial}{\partial x}(G * d(x, y, t)) \\ \frac{\partial}{\partial y}(G * d(x, y, t)) \end{pmatrix}$$

as the potential generated by obstacles. We select the parameter σ to be half the image size.

3.2 Optical Flow as Attractive Force

From the geometric properties of flow field and the potential, we define potential field $\boldsymbol{p}(x, y, t)$ as

$$\boldsymbol{p}(x, y, t) = \begin{cases} \boldsymbol{g}(x, y, t) - \hat{\boldsymbol{u}}(x, y, t), \text{ if } d(x, y, t) = 255 \\ \boldsymbol{g}(x, y, t), \qquad\qquad \text{otherwise} \end{cases}.$$

The gradient vector field $\boldsymbol{g}(x, y, t)$ is a repulsive force from obstacles. The planar flow field $\hat{\boldsymbol{u}}(x, y, t)$ as an artificial attractive force to the destination.

Proceedings of the 5th International Conference on Computer Vision Systems (ICVS 2007)
Published in 2007 by Applied Computer Science Group, Bielefeld University, Germany, ISBN 978-3-00-020933-8
This document and other contributions archived and available at: http://biecoll.ub.uni-bielefeld.de

Since the planar flow $\hat{\boldsymbol{u}}(x, y, t)$ represents the camera motion, the sum of the sign-inversed planar flow field $-\hat{\boldsymbol{u}}(x, y, t)$ and the gradient vector field $\boldsymbol{g}(x, y, t)$ is the potential field $\boldsymbol{p}(x, y, t)$. However, in the obstacle area in an image, the planar flow field $\hat{\boldsymbol{u}}(x, y, t)$ is set to zero, since the planar flow field represents the dominant plane motion. If obstacles do not exist in an image, the above equation becomes

$$\boldsymbol{p}(x, y, t) = \hat{\boldsymbol{u}}(x, y, t). \tag{6}$$

Then, the robot moves forward according to the planar flow field.

3.3 Navigation of Nonholonomic Mobile Robot by Potential Field

We define the control force $\bar{\boldsymbol{p}}(t)$ using the average of the potential field $\boldsymbol{p}(x, y, t)$ as

$$\bar{\boldsymbol{p}}(t) = \frac{1}{|A|} \int_{(x,y)^\top \in A} \boldsymbol{p}(x, y, t) dx dy, \tag{7}$$

where $|A|$ is the size of the region of interest in an image captured by the camera mounted on the mobile robot.

Since we apply the control force $\bar{\boldsymbol{p}}(t)$ to the nonholonomic mobile robot, we require that the control force is transformed into the translational velocity and rotational velocity. We determine the ratio between the translational and rotational velocity using the angle of the control force $\bar{\boldsymbol{p}}(t)$.

We assume that the camera mounted on the mobile robot captures an image in front of the mobile robot. Therefore, we set parameter $\theta(t)$ to be the angle between the control force $\bar{\boldsymbol{p}}(t)$ and the y axis $\boldsymbol{y} = (0, 1)^\top$ of the image, which is the forward direction of the mobile robot, as shown in Fig. 2. That is,

$$\theta(t) = \arccos \frac{\langle \bar{\boldsymbol{p}}(t), \boldsymbol{y} \rangle}{|\bar{\boldsymbol{p}}(t)||\boldsymbol{y}|}. \tag{8}$$

In Fig. 2(Middle), we show the relationships among $\bar{\boldsymbol{p}}(t)$, $\theta(t)$, and the direction of robot motion.

We define robot translational velocity $T(t)$ and rotational velocity $R(t)$ at time t as

$$T(t) = T_m \cos\theta(t), \quad R(t) = R_m \sin\theta(t), \tag{9}$$

where T_m and R_m are the maximum translational and rotational velocity of the mobile robot between time t and $t + 1$. Setting $\boldsymbol{X}(t) = (X(t), Y(t))^\top$ to be the position of robot at time t in the world coordinate system, from Eq. (9), we have the relations,

$$\sqrt{\dot{X}(t)^2 + \dot{Y}(t)^2} = T(t), \quad \tan^{-1} \frac{\dot{Y}(t)}{\dot{X}(t)} = R(t). \tag{10}$$

Proceedings of the 5th International Conference on Computer Vision Systems (ICVS 2007)
Published in 2007 by Applied Computer Science Group, Bielefeld University, Germany, ISBN 978-3-00-020933-8
This document and other contributions archived and available at: http://biecoll.ub.uni-bielefeld.de

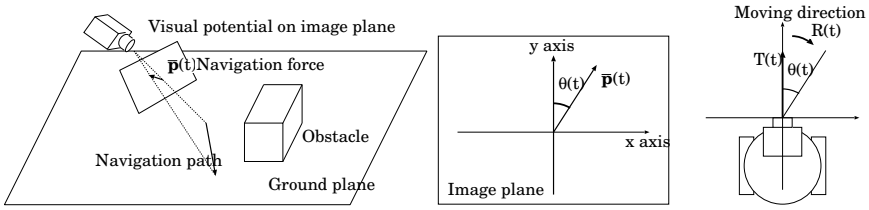

Fig. 2. Navigation from potential field. (Left) Navigation force $\bar{\boldsymbol{p}}(t)$ is the local navigation path. (Middle) The angle between the control force $\bar{\boldsymbol{p}}(t)$ and y axis is $\theta(t)$. (Right) Robot displacement $T(t)$ and rotation angle $R(t)$ at time t are determined using $\theta(t)$.

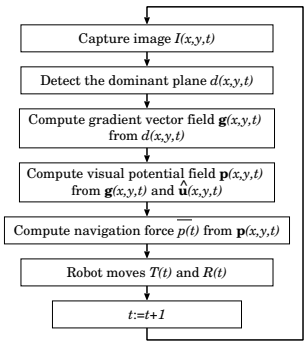

Fig. 3. Closed loop for autonomous robot motion. Computations of $g(x, y, t)$, $p(x, y, t)$, and $T(t)$ and $R(t)$ are described in sections 3.1, 3.2, and 3.2, respectively. The algorithm for the detection of dominant plane d is described in section 2.

Therefore, we have the control law

$$\dot{X}(t) = T(t) \cos R(t), \tag{11}$$

$$\dot{Y}(t) = T(t) \sin R(t). \tag{12}$$

The relations form Eq. (1) to Eq. (12) are symbolically expressed as

$$\dot{\boldsymbol{X}}(t) = f(I_t, I_{t-1}, I_{t-2}), \tag{13}$$

since the visual potential on I_t is computed from images I_t, I_{t-1}, and I_{t-2}. The algorithm for the navigation of the mobile robot based on Eq. (13) is shown in Fig. 3.

4 Experimental Results

We show collision avoidance of the mobile robot using our algorithm in the real environment. The specifications of the mobile robot are described in Table 1.

Proceedings of the 5th International Conference on Computer Vision Systems (ICVS 2007)
Published in 2007 by Applied Computer Science Group, Bielefeld University, Germany, ISBN 978-3-00-020933-8
This document and other contributions archived and available at: http://biecoll.ub.uni-bielefeld.de

The environments for the experiment are the straight and curved pathway. In these environments, the robot moved without collision to obstacles and wall s of the corridor.

The experimental results for the straight pathway, the curved pathway in counterclockwise direction, and the curved pathway in clockwise direction are shown in Figs. 4, 5, and 6, respectively. In these figures, the top row shows snapshots of the experiment. In the middle row, starting from the left, the captured image $I(x, y, t)$, the estimated optical flow field $(\dot{x}, \dot{y})^\top$, and the detected dominant plane $d(x, y, t)$ at a frame are shown. In the detected dominant plane, the white and black colored regions represent the dominant plane and the obstacle, respectively. In the bottom row, starting from the left, the gussian-operated image $G * d(x, y, t)$, the potential field $\boldsymbol{p}(x, y, t)$, and the estimated control force $\bar{\boldsymbol{p}}(t)$ at a frame are shown.

Figure 4 shows that the estimated control force in the straight pathway indicates forward direction. Therefore, the robot moves forward direction. Figure 5 shows that the estimated control force in the counterclockwise pathway indicates left direction. Therefore, the robot rotates in the counterclockwise direction. Figure 6 shows that the estimated control force in the clockwise pathway indicates right direction. Therefore, the robot rotates in the clockwise direction. These results show that our algorithm enables the mobile robot to move without collision with obstacles without any pre-determined robot trajectories and environmental maps.

Table 1. Specifications of our mobile robot

Name	Magellan Pro, AAI Systems, Inc.
Size	Circular - 16-inch diameter
Weight	50 pounds
Drive	2-wheel
CPU	800MHz, AMD-K6 processor
Main memory	256MB
OS	Red Hat Linux
Compiler	GNU C++ Compiler
Camera	SONY EVI-D30

5 Conclusions

We developed an algorithm for the navigation of an autonomous mobile robot using the visual potential field. Our method enables a mobile robot to avoid obstacles without the need for an environmental map. Experimental results show that our algorithm is robust against the fluctuation of the displacement of the mobile robot.

Proceedings of the 5th International Conference on Computer Vision Systems (ICVS 2007)
Published in 2007 by Applied Computer Science Group, Bielefeld University, Germany, ISBN 978-3-00-020933-8
This document and other contributions archived and available at: http://biecoll.ub.uni-bielefeld.de

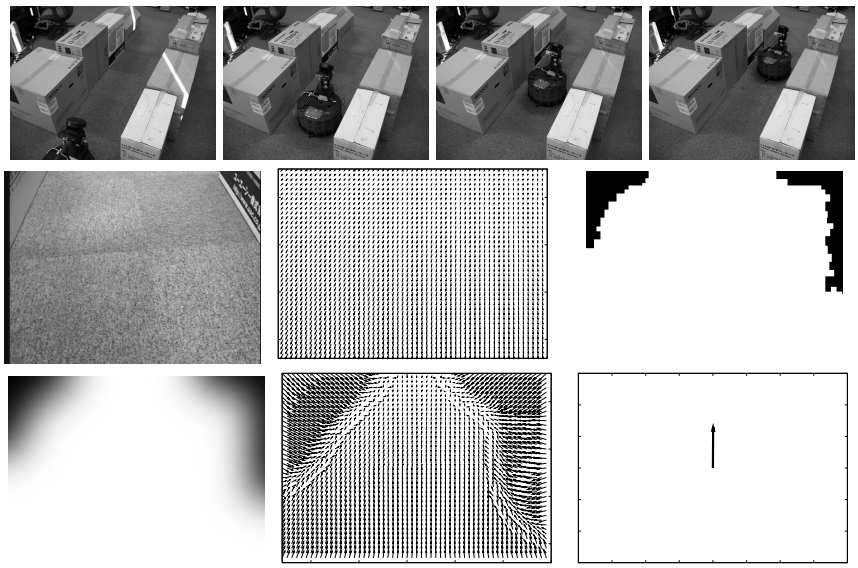

Fig. 4. Experimental result for the straight pathway. The images in top row are snapshots of this experiment. In the middle row, starting from the left, captured image $I(x, y, t)$, estimated optical flow field $(\dot{x}, \dot{y})^\top$, and detected dominant plane $d(x, y, t)$ at a frame. In the bottom row, starting from the left, gussian image $G*d(x, y, t)$, potential field $\boldsymbol{p}(x, y, t)$, and estimated control force $\bar{\boldsymbol{p}}(t)$ at a frame.

The visual potential field used for guiding the robot is generated from visual information captured with a camera mounted on the robot without the use of any maps that describe the workspace. We presented that optical flow vectors indicate the direction of robot motion to the local destination. Therefore, the optical flow field is suitable for the guide field to the destination of the robot. Furthermore, we generated a potential field of anti-attraction force from obstacles to avoid collision, using images captured with the camera mounted on the robot. Using this field as the guidance field for the robot navigation, the robot selects a corridor path to the local goal. This local corridor path computed from images can be used in the navigation of a mobile robot.

References

1. Aarno, D., Kragic, D., and Christensen, H.I.: Artificial potential biased probabilistic roadmap method. ICRA'04, **1** (2004) 461–466
2. Barron, J.L., Fleet, D.J., and Beauchemin, S.S.: Performance of optical flow techniques. Int. J. of Computer Vision, **12** (1994) 43-77
3. Bouguet, J.-Y.: Pyramidal implementation of the Lucas Kanade feature tracker description of the algorithm. Intel Corporation, Microprocessor Research Labs, OpenCV Documents, (1999)

Proceedings of the 5th International Conference on Computer Vision Systems (ICVS 2007)
Published in 2007 by Applied Computer Science Group, Bielefeld University, Germany, ISBN 978-3-00-020933-8
This document and other contributions archived and available at: http://biecoll.ub.uni-bielefeld.de

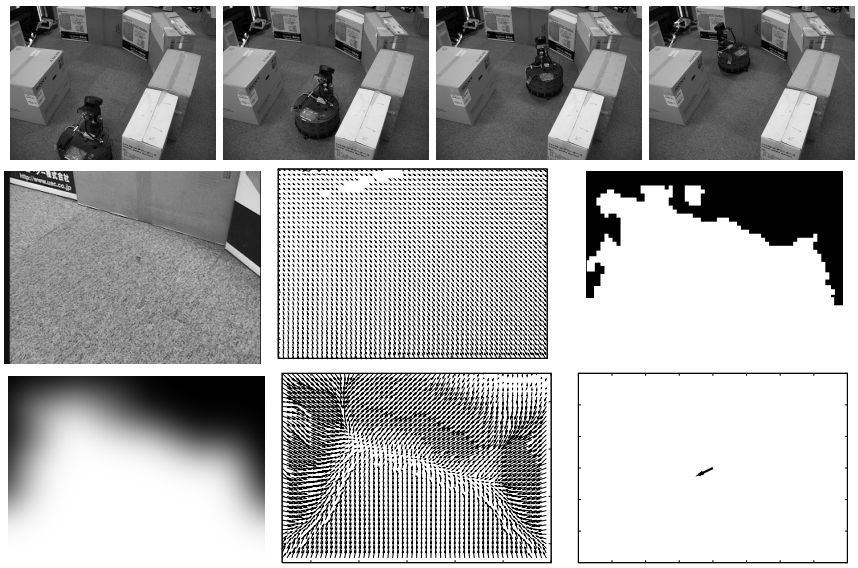

Fig. 5. Experimental result for the curved pathway in counterclockwise direction. The snapshots, captured image, and the results are shown.

4. Capparella, F., Freda, L., Malagnino, M., and Oriolo, G.: Visual servoing of a wheeled mobile robot for intercepting a moving object. IROS'05 (2005) 2021–2027
5. Conner, D.C., Rizzi, A.A., and Choset, H.: Composition of local potential functions for global robot control and navigation. Int. Conf. on Intelligent Robots and Systems, **4** (2003) 3546–3551
6. Das, A., Fierro, R., Kumar, V., Southall, J., Spletzer, J., and Taylor, C.: Real-time vision-based control of a nonholonomic mobile robot. ICRA'01 (2001) 1714–1719
7. Fischler, M.A. and Bolles, R.C.: Random sample consensus: A paradigm for model fitting with applications to image analysis and automated cartography. Comm. of the ACM, **24** (1981) 381–395
8. Guilherme, N.D. and Avinash, C.K.: Vision for mobile robot navigation: A survey. IEEE Trans. on PAMI, **24** (2002) 237–267
9. Hartley, R., and Zisserman, A.: *Multiple View Geometry in Computer Vision*. Cambridge University Press, (2000)
10. Horn, B.K.P. and Schunck, B.G.: Determining optical flow. Artificial Intelligence, **17** (1981) 185–203
11. Khatib, O.: Real-time obstacle avoidance for manipulators and mobile robots. Int. J. of Robotics Research, **5** (1986) 90–98
12. Lucas, B. and Kanade, T.: An iterative image registration technique with an application to stereo vision. Int. Joint Conf. on Artificial Intelligence, (1981) 674–679
13. Ma, Y., Kosecka, J., and Sastry, S.S.: Vision guided navigation for a nonholonomic mobile robot. IEEE Transactions on Robotics and Automation, **15** (1999) 521–536
14. Mnif, F. and Touati, F.: An Adaptive Control Scheme for Nonholonomic Mobile Robot with Parametric Uncertainty. Int. J. of Advanced Robotic Systems, **2** (2005) 59-63

Proceedings of the 5th International Conference on Computer Vision Systems (ICVS 2007)
Published in 2007 by Applied Computer Science Group, Bielefeld University, Germany, ISBN 978-3-00-020933-8
This document and other contributions archived and available at: http://biecoll.ub.uni-bielefeld.de

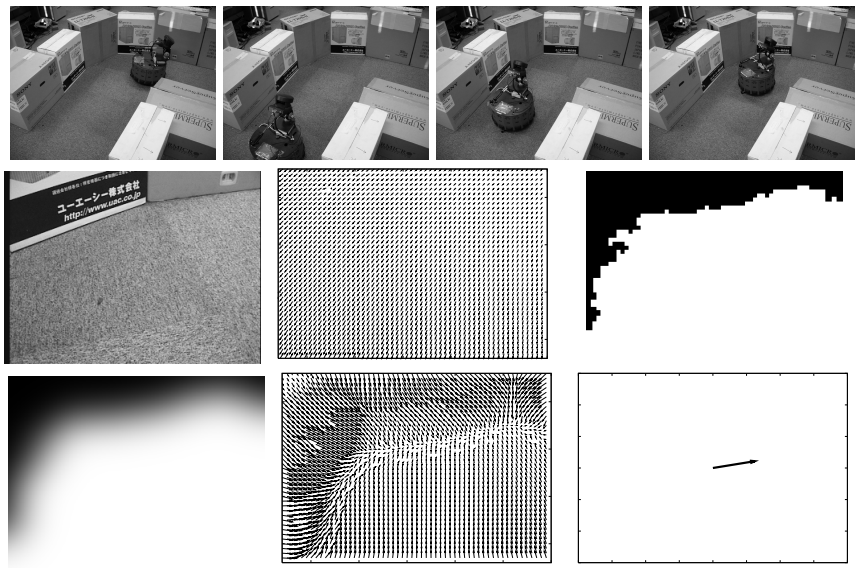

Fig. 6. Experimental result for the curved pathway in clockwise direction. The snapshots, captured image, and the results are shown.

15. Nagel, H.-H. and Enkelmann, W.: An investigation of smoothness constraint for the estimation of displacement vector fields from image sequences. IEEE Trans. on PAMI, **8** (1986) 565–593
16. Ohnishi, N. and Imiya, A.: Featureless robot navigation using optical flow. Connection Science, **17** (2005) 23–46
17. Ohnishi, N. and Imiya, A.: Dominant plane detection from optical flow for robot navigation. Pattern Recognition Letters, **27** (2006) 1009–1021
18. Shimoda, S., Kuroda, Y., and Iagnemma, K.: Potential field navigation of high speed unmanned ground vehicles on uneven terrain. ICRA'05 (2005) 2839–2844
19. Tews, A.D., Sukhatme, G.S., and Matarić, M.J.: A multi-robot approach to stealthy navigation in the presence of an observer. ICRA'04 (2004) 2379–2385
20. Trihatmo, S. and Jarvis, R. A.: Short-safe compromise path for mobile robot navigation in a dynamic unknown environment. Australian Conf. on Robotics and Automation, (2003).
21. Valavanis, K., Hebert, T., Kolluru, R., and Tsourveloudis, N.: Mobile robot navigation in 2D dynamic environments using an electrostatic potential field. IEEE Trans. on Systems, Man, and Cybernetics, **30** (2000) 187–196
22. Wada, N., Saeki, M., and Chen, H.: Robust Tracking Control of a Nonholonomic Mobile Robot in the Presence of Disturbances. JSME Int. J. Series C, **47** (2004) 694–701

Proceedings of the 5th International Conference on Computer Vision Systems (ICVS 2007)
Published in 2007 by Applied Computer Science Group, Bielefeld University, Germany, ISBN 978-3-00-020933-8
This document and other contributions archived and available at: http://biecoll.ub.uni-bielefeld.de